



## Vapour compression refrigeration with biomass operated bubble column humidification and dehumidification desalination system

K. Srithar<sup>a,\*</sup>, R. Saravanan<sup>b</sup>, R. Srinivasan<sup>c</sup>, T. Rajaseenivasan<sup>d</sup>, R. Venkatesan<sup>c</sup>,  
A. Mariganesh<sup>a</sup>, K.N. Aravinth<sup>a</sup>

<sup>a</sup>Department of Mechanical Engineering, Thiagarajar College of Engineering, Madurai – 625 015, India,  
emails: ponsathya@hotmail.com (K. Srithar), mariganesh1211@gmail.com (A. Mariganesh),  
knaravinthnatarajan@gmail.com (K.N. Aravinth)

<sup>b</sup>Department of Mechanical Engineering, College of Engineering–Guindy Campus, Anna University, Chennai – 600 025,  
India, email: paramsrinivasan@gmail.com

<sup>c</sup>Department of Mechanical Engineering, R.V.S. College of Engineering, Dindigul – 624 005, India,  
emails: rsaravanan@annauniv.edu (R. Saravanan), r.venkatharan1986@gmail.com (R. Venkatesan)

<sup>d</sup>Department of Mechanical Engineering, University of California Merced, Merced, California – 95343, USA,  
email: trseenivasan@gmail.com

Received 24 March 2020; Accepted 2 December 2020

---

### ABSTRACT

This work focuses on the performance augmentation in a vapor compression refrigeration (VCR) system integrated with biomass operated bubble column humidification–dehumidification desalination unit. The saline water supplied to the bubble column humidifier is preheated while passing around the condenser of the VCR system. It is a sub-cooling process that leads to more heat rejection to surrounding and further increases the coefficient of performance (COP). The saline water and air from the blower are then heated by biomass energy in the bubble column humidifier and the air gets humidified and sent to a dehumidifier. A dehumidifier is a triple pipe heat exchanger where the refrigerant flows in the inner pipe which flows between the evaporator and compressor of the VCR. Humid air from the humidifier flows at the middle pipe and the saline water flows in the outermost pipe. As the humid air in contact with both cold refrigerant and saline water, moist air is condensed, and the pure water is collected. It is found that the distillate output and COP of the VCR unit increase with air mass flow rate, water depth and temperature in the humidifier. Theoretical results of specific humidity of air outlet from the humidifier are validated with experimental work within 10% deviation. The distilled water cost of 0.067 \$/kg and the gained output ratio ranges between 0.286 and 0.388 for the proposed system.

*Keywords:* Desalination; Vapor compression refrigeration; Waste heat recovery; Humidification–dehumidification desalination; Biomass desalination

---

### 1. Introduction

The refrigeration and heating, ventilation and air conditioning (HVAC) industry play a foremost role in today's global economy. The HVAC sector consumes about 17% of the overall electricity consumed worldwide. So, the

performance of the refrigeration system should be improved for reducing the consumption of electricity and thereby control global warming. Gao et al. [1] studied the humidification–dehumidification (HDH) desalination integrated with a vapour compression heat pump. The heat from the condenser is used for humidification of air in the humidifier

---

\* Corresponding author.

and cold from the evaporator is used to absorb heat from moist air passing through the dehumidifier chamber. It was observed that the desalination unit considered in that study produced the distillate of 60 kg/d with the use of less energy consumption in the compressor (500 W). Lokapure and Joshi [2] developed a multi-utility air conditioning system to produce air conditioning effects along with the generation of hot water by absorbing heat from the condenser. The coefficient of performance (COP) of the air-conditioner increased by 13.66%. Wang et al. [3] recovered the waste heat from the condenser of a vapor compression refrigeration system and the same was supplied to the generator of the vapor absorption refrigeration system. The hybrid refrigeration system was found to recover all the condensation heat. Chinguwa et al. [4] improved the COP of the cool box for passenger cars by means of using a thermoelectric refrigeration system. DC power for this thermoelectric refrigeration system is produced by a thermoelectric generator that absorbs waste heat from the passenger car. Raveendran and Sekhar [5] studied the domestic refrigerator with the water-cooled condenser. The obtained results showed that the COP of the system with brazed plate heat exchanger as the water-cooled condenser is 57% to 75% higher than that of the air-cooled condenser. Javani et al. [6] recovered waste heat in a hybrid electric vehicle and used it for cooling the cabin. The result shows that transferring this waste heat to the boiler in the ejector cooling system leads to a cooling effect of 7.23 kW. Nada et al. [7] used the waste heat retrieved from the air conditioner for HDH desalination.

It is inferred that an increase in specific humidity and the air-flow rate which in turn augments the freshwater output, the refrigeration capacity and reduction in compressor work per kg of freshwater. Srithar et al. [8] recovered waste heat from the condenser and evaporator of the VCR system, which was used for HDH desalination. Air passed in counter flow direction in the humidifier absorbed the moisture and this moist humid air was condensed in dehumidifier cooled outlet coil from the evaporator of the same VCR system. From the study, COP is increased about 2.09 times greater than a conventional refrigerator.

Kabeel et al. [9] carried out an experimental investigation on HDH desalination using various types of cellulose papers as packing materials in the humidifier chamber. An open-air and closed water circuit was employed in this system. Modified dehumidifier design increases the effectiveness up to 0.71 while conventional dehumidifier yields only 0.49. Mohamed and El-Minshawy [10] presented a humidification and dehumidification process that is supplied with hot seawater by geothermal energy. The various mass flow rate of seawater has been tried and fixed to the optimum ranges. A thermodynamic study on an HDH system driven by a parabolic solar collector was conducted by Al-Sulaiman et al. [11]. An air-heated HDH desalination system with plate heat exchangers to recover the waste heat from the exhaust gas was conducted by He et al. [12]. Results showed that once the top temperature is reached, waste heat recovery and the distilled water production were reduced.

Behnam et al. [13] examined a solar power desalination system equipped with a heat pipe for heating saline water in the bubble column humidifier. Effects of various parameters including incoming air-flow rate into the

humidifier, initial depth of water in the humidifier and adding fluids in the heat pipe such as oil and water in spaces were investigated. Srithar and Rajaseenivasan [14] carried out an experimental work to analyze the effect of direct and preheated air supply by a solar air heater in a bubble column humidifier. Different turbulators were used to enhance the humidification. Solar hybrid air conditioning and HDH water desalination system were presented by Elattar et al. [15]. It was inferred that the total operating cost increases with increasing outdoor air temperature and outdoor humidity and decreases with increasing temperature difference across the heating system. Rajaseenivasan and Srithar [16] described a biomass powered bubble column humidification–dehumidification desalination system. Better specific humidity is recorded with a bubble pipe-hole diameter of 1 mm, water depth of 170 mm and a water temperature of 60°C. The highest distillate of 6.1 and 3.5 kg/h is collected for the HDH desalination system with preheated air and direct air supply respectively.

Triple pipe heat exchanger is a device that exchanges the heat between three fluids. Now, researchers are continuously studying the performance improvement in the triple pipe heat exchanger. Rdulescu et al. [17] experimented first with a tube in the tube heat exchanger and then with a triple concentric tube heat exchanger (TCTHE) for the same operating conditions. It has been concluded that heat flow rates for the same unit length, the heat transfer area and overall heat transfer coefficients are higher for TCTHE. Quadir et al. [18] fabricated a triple concentric pipe heat exchanger and investigated the heat exchange behavior between three fluids under different operating conditions. In N–H–C arrangement, cold water flowing (C) in the innermost pipe, hot water (H) flowing in the inner annulus, and normal water (N) flowing in the outer annulus. The authors inferred that the heat transfer rate is not considerably affected by the external environment. Gomma et al. [19] investigated a triple pipe heat exchanger having inserted ribs in the inner pipe with a C–H–N arrangement. Results show that the effectiveness of the ribbed pipe is higher than the pipe without ribs by 17.65% (parallel flow) and 16.2% (counter flow). Observed results show that increasing the number of ribs results in an increase in heat transfer coefficient by 15.7%. From these articles, the triple pipe heat exchanger is far better than a double pipe heat exchanger.

Recently, Lawal et al. [20] have theoretically analyzed a heat pump operated humidification–dehumidification desalination unit by changing the various parameters in both systems. The increase in humidifier and dehumidifier effectiveness considerably augments the system gained output ratio. Lawal et al. [21] have experimentally studied a heat pump-operated humidification–dehumidification desalination system for space conditioning and freshwater production. A maximum gained output ratio of 4.07 is achieved and the COP of the heat pump ranges between 3.06 and 4.86. Anand and Murugavelh [22] have tested the VCR integrated humidification–dehumidification desalination. The combined system resulted in a distilled yield of 7.5 l/h and cooling output of 1.89 kW. Faegh et al. [23] have reviewed the research works conducted on the humidification–dehumidification desalination-based refrigeration, power and multi-generation cycles. Also,

reported the HDH cycles integrated with various desalination methods. Lawal and Qasem [24] have reviewed the research works performed in the HDH desalination that is driven by renewable and low-grade energy sources. It has been reported that the integration of refrigeration system leads to the higher gained output ratio.

From the literature survey, most of the studies were done for recovering waste heat on the air-conditioning system and VCR system. Waste heat from the condenser unit of such devices was retrieved and used for heating water. Few works have been carried out so far, to recover the heat energy from the condenser and evaporator of the VCR system and utilize this energy for desalination system and leaving a research gap of integrating the VCR with biomass-based HDH desalination.

Also, a triple pipe heat exchanger is introduced to (i) enhance the VCR performance by super-heating the refrigerant, (ii) augment the distillation rate by using low-temperature refrigerant as cold fluid, and (iii) preheating the saline water from hot humid air. These types of heat recovery arrangements are new and beneficial to all the fluids involved in the heat exchanging process. Most of the waste energy is effectively used to improve the performance of the overall system rather than releasing the waste heat to the atmosphere. Biomass is used as the thermal energy source for the desalination system. The experiments are conducted by varying the air-flow rate, water depth in bubble column humidifier, and bubble column water temperature.

## 2. Experimental setup

The experimental setup mainly consists of a biomass stove, humidifier, dehumidifier and refrigeration unit. The schematic and photographic view of the overall setup is shown in Figs. 1 and 2. A commercial refrigerator with a

cooling capacity of 480 W and a capacity of 400 L is used in this study (R-134 as a refrigerant).

Biomass stove is made up of sheet metal having two components such as burning chamber and ash collecting chamber and its dimensions are 0.28 m × 0.28 m × 0.35 m (Fig. 3). Two connections are given to the biomass stove from the blower. Primary air is supplied from a blower and this air is used only for burning the fuel. Separate provision (hopper) is made in the burning chamber which is used for biomass feeding. The main purpose of a biomass stove is to heat the saline water. At the same time, it is also used for preheating the air which enters the humidifier. The biomass stove is painted with red oxide to avoid corrosion. Charcoal is used as burning fuel for experimental purposes (calorific value – 29,600 kJ/kg). Two holders are provided for carrying the biomass stove. Four 5 mm thickness strips are used for the proper placing of bubble column humidifier on the biomass stove. Ash produced when burning the fuel is separately collected in the chamber which is located at the bottom of the stove.

A humidifier is a rectangular box with a size of 0.28 m × 0.28 m × 0.5 m. It has two inlets; one belongs to water and another one belongs to air and it has one outlet for hot moist air. This bubble column humidifier has two-layer spider spargers (Fig. 4). Each sparger has two arms and each arm has 50 holes of 2 mm diameter. The bubble column humidifier has a top cover inclined with an angle of 45° to collect this condenser water. The condensate is collected by a small opening provided on the back face of the bubble column humidifier.

A dehumidifier is a triple pipe heat exchanger where refrigerant vapor from the evaporator of the refrigerator flows in an innermost pipe, hot moist air flows in the inner annulus and water flow in the outer annulus. The inner pipe is fabricated using a copper tube of 0.006 m diameter

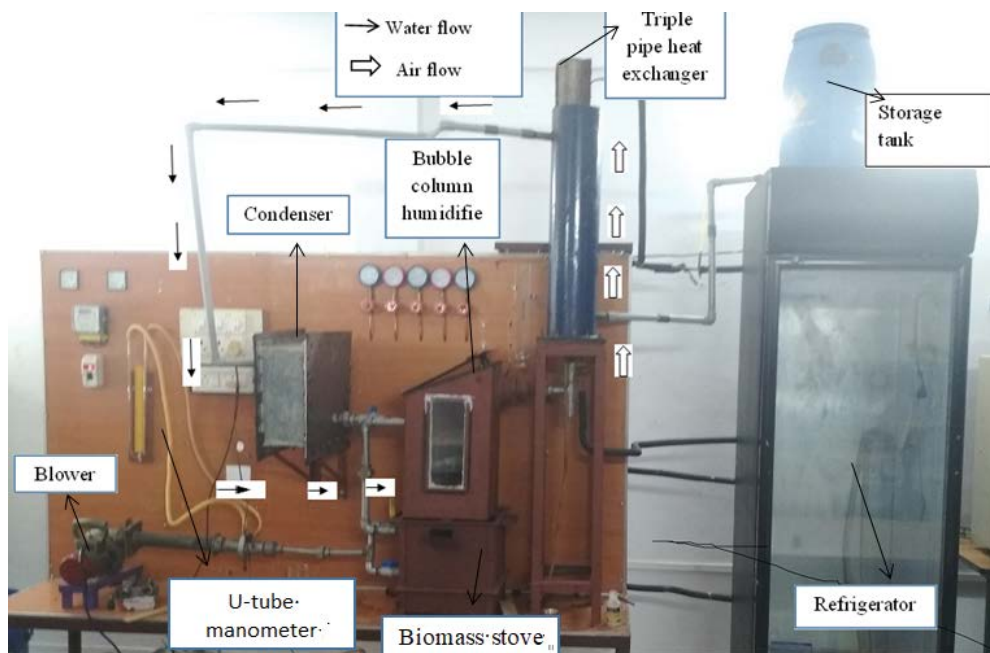


Fig. 1. A photographic view of the experimental setup.

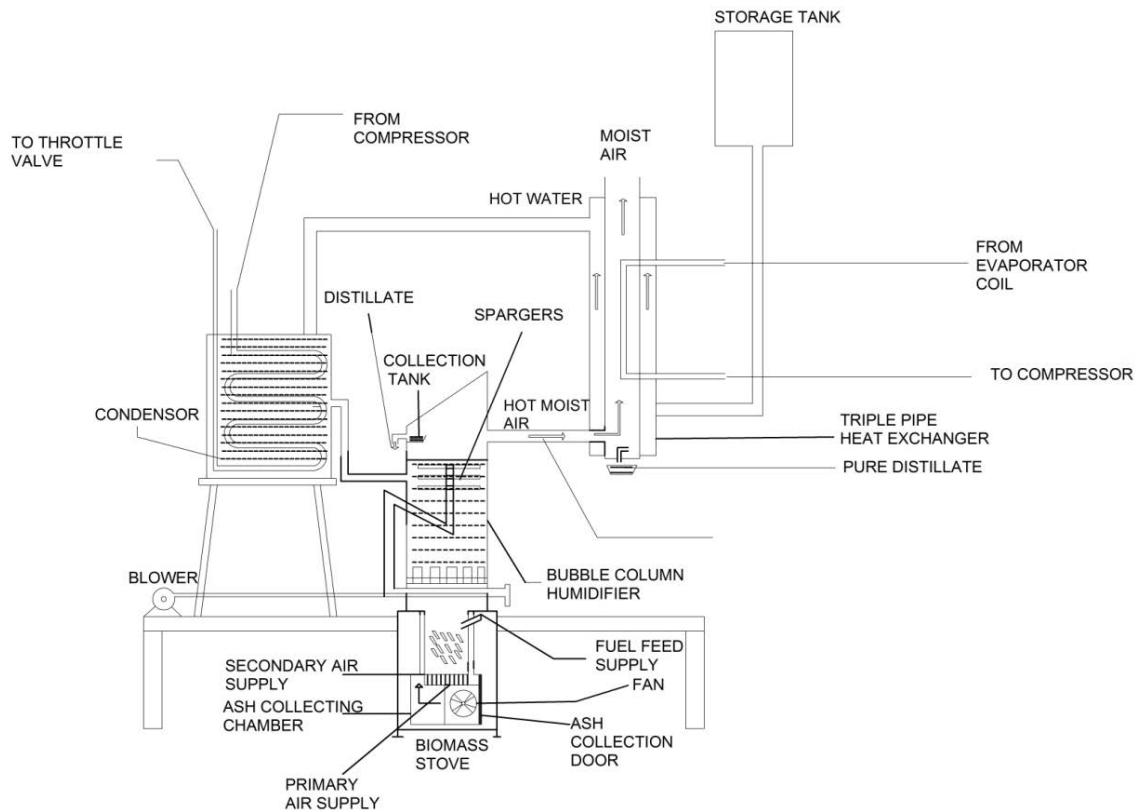


Fig. 2. A sectional view of the overall system.

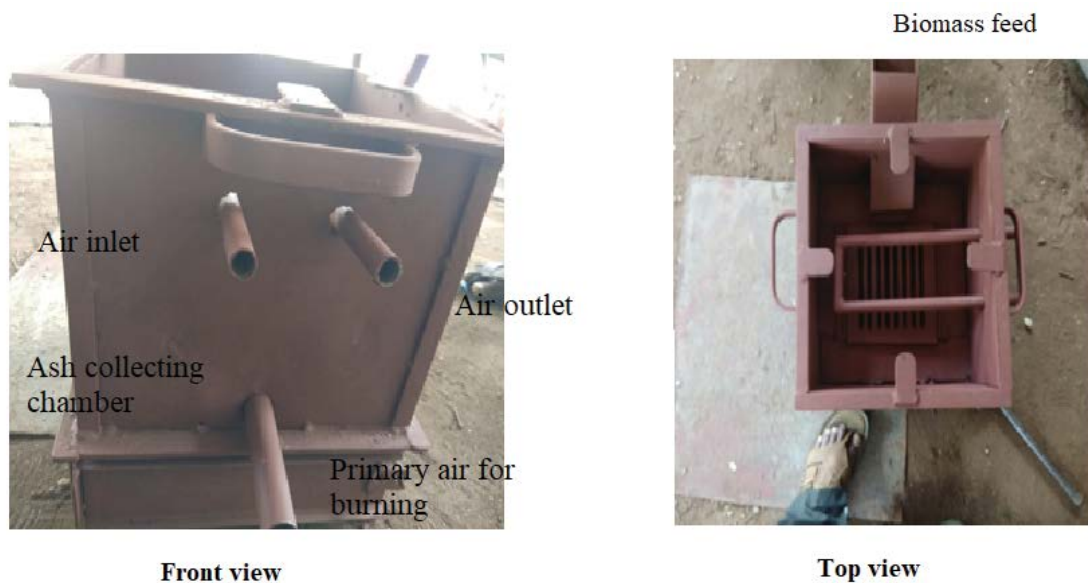


Fig. 3. A photographic view of the biomass stove.

and it is wound into the inner diameter of 0.045 m of 60 turns having a length of 0.06 m. This copper coil is placed in between the two half-pipes of the GI pipe of diameter 0.09 m and a height of 0.9 m. Small inserts have attached to this pipe to resist the flow of air. They are square (30 mm × 30 mm) in a shape of the thickness of 5 mm and a total of 45 inserts

are used (Fig. 5). The outermost pipe is made up of GI having a diameter of 0.152 m and a length of 0.75 m. The inlet of the outermost pipe is connected to the storage tank. The outlet of this pipe is connected to the condenser chamber.

Initially, the saline water enters the outer pipe of the triple pipe heat exchanger (dehumidifier). Here, the saline



Fig. 4. A photographic view of the spargers and bubble formation in the humidifier.

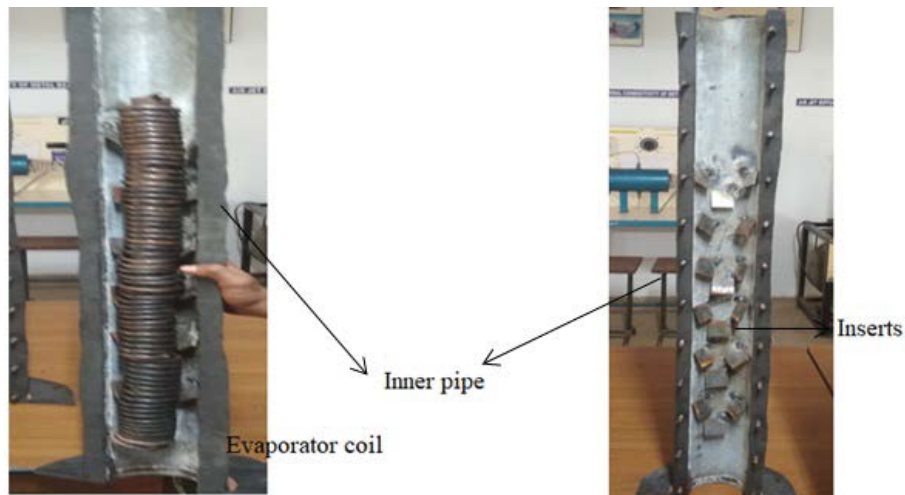


Fig. 5. A photographic view of the dehumidifier.

water absorbs the heat from the hot humid air which is passing in the middle pipe. Then enters another heat exchanger (condenser for refrigerant from refrigerator compressor) where the saline water is further heated by absorbing the heat from the refrigerant and condenses the refrigerant. The condenser tube is covered with a box (made up of a sheet of 3 mm thickness) of dimensions of  $0.35\text{ m} \times 0.35\text{ m} \times 0.15\text{ m}$ . This preheated saline water is supplied to the bubble column humidifier. The humidifier is placed over the stove where it is heated to the desired water temperature.

A blower is used to supply the air required for the processes. Two connections are given to the biomass stove from the blower. Primary air is also supplied from the blower. This air is used only for burning the fuel. The air is first preheated in the biomass stove and then enters the humidifier through spargers. As the heated air is passed through the holes of the spargers which are immersed in the hot saline water bath, the air gets humidified and moves up to the top of the surface due to density difference. Some of the moist air is condensed on the top surface of the humidifier and most of the moist air is leaving the dehumidifier chamber. The humid air passes in the middle pipe where it loses the heat to the refrigerant in the inner

pipe and the saline water in the outer pipe. The moist air from the humidifier chamber enters the middle pipe of the triple pipe heat exchanger. The inner pipe of the dehumidifier is the evaporator exit coil of the refrigerator, in the middle pipe moist air flows up from the bottom side to the top side and in the outer coil saline water from the storage tank flows by gravity as shown in Fig. 2. The moist air left off its heat on both the fluid and thus distillation is collected at the bottom. At the same time as the refrigerant gets super-heated and enters the refrigerator compressor.

At first, the refrigerator is allowed to run in the conventional model, without a desalination unit and the readings have been noted. Then experiments are continued with the desalination system and the temperature of moist air at humidifier inlet, humidifier outlet, dehumidifier outlet, condenser inlet and condenser outlet are noted based on the variation in the mass flow rate of inlet air for four readings at a constant water temperature of  $50^\circ\text{C}$  in a humidifier with a depth of 0.10 and 0.20 m for a span of 20 min. Water temperature is maintained by means of adjusting fuel supply in the biomass stove. The COP is also determined for the various temperature of water in the humidifier and various depths of 0.10 and 0.20 m.

Meanwhile, the pressure drop across the evaporator inlet, evaporator outlet, dehumidifier outlet, condenser inlet and condenser outlet also noted for determining the COP of the refrigeration system. A separate measuring jar of 1 L is used for collecting and measuring the distillate produced.

### 3. Data reduction

The performance of refrigeration systems and heat pumps is indicated by its COP. The COP is defined by the ratio of the amount of useful cooling at the evaporator ( $Q$ ) to the compressor work input required for running the device ( $W$ ).

$$\text{COP} = \left( \frac{Q}{W} \right) \quad (1)$$

Theoretical refrigerating effect capacity and compressor work can be expressed in terms of enthalpy are indicated in Eq. (2).

$$\text{COP} = \left( \frac{h_1 - h_4}{h_2 - h_1} \right) \quad (2)$$

In a bubble column humidifier, preheated air that comes through the bubble hole is mixed with hot water available in a humidifier. The temperature and concentration difference between air and water causes sensible and latent heat transfer between air and water. Here, water temperature is held at constant by properly maintaining the burning rate. The energy balance equation can be written as:

$$\dot{E}_{\text{in}} - \dot{E}_{\text{out}} = \dot{E}_{\text{stored}} \quad (3)$$

Because of very small size of air bubble the energy stored in the air bubble is assumed to be negligible. So, it can be rewritten as:

$$\dot{E}_{\text{in}} = \dot{E}_{\text{out}} \quad (4)$$

Energy balance equation is also written in terms of enthalpy for the humidification process as:

(Enthalpy of inlet air) + (Sensible heat from water to air bubble) + (Latent heat from water to air bubble) = (Enthalpy of outlet air).

$$\dot{m}_a H_1 + \dot{E}_{\text{sen}} + \dot{E}_{\text{lat}} = \dot{m}_a H_2 \quad (5)$$

where  $H$  is the enthalpy of air which can be calculated as:

$$H = C_p T + \omega h_g \quad (6)$$

Sensible heat transfer can be derived by the relation by considering water height in humidifier ' $Z$ ' (m), specific interfacial area of the bubble ' $a$ ' (1/m) and area of water ' $A$ ' (m<sup>2</sup>) with the heat transfer coefficient ' $h$ ' (kW/m<sup>2</sup>K) for the given temperature difference.

$$\dot{E}_{\text{sen}} = hA(T_w - T_a) a Z \quad (7)$$

The specific interfacial area is the bubble surface area in the bubble column and it is determined by the following relation [16].

$$a = \frac{6\varepsilon}{d_b} \quad (8)$$

where  $\varepsilon$  is the gas holdup, that is defined as the volume fraction of the gas-phase occupied by gas bubbles and shown as follows [16]:

$$\varepsilon = \frac{V_g}{0.3 + 2V_g} \quad (9)$$

where  $V_g$  is the superficial velocity which is obtained by dividing the mass flow rate of air by bubble column surface area. Bubble diameter  $d_b$  is given by the following relation [16]:

$$d_b = \left[ \frac{6\sigma d_0}{g(\rho_w - \rho_a)} \right]^{1/3} \quad (10)$$

Latent heat transfer for the given specific humidity difference can be obtained by considering the mass transfer co-efficient  $h_d$  (kg/m<sup>2</sup> s) with the latent heat of vaporization (kJ/kg), water surface area (m<sup>2</sup>), water height  $Z$  (m) and specific interfacial area  $a$  (1/m) of the bubble.

$$\dot{E}_{\text{lat}} = h_d (\omega_v - \omega_a) h_{fg} a Z \quad (11)$$

Lewis factor is used to relate heat and mass transfer co-efficient by:

$$\text{Le} = \frac{h}{h_d C_p} \quad (12)$$

Substituting Eqs. (7), (11), and (12) in Eq. (6) and this equation is further reduced by considering  $\text{Le} = 1$  [16], we can get an equation in terms of enthalpy of outlet air. By interpolating enthalpy of outlet air, corresponding specific humidity and temperature can be found out.

$$H_2 = \left[ \frac{h_d a A (h_f - C_p T)}{\dot{m}_a} \right] + H_1 \quad (13)$$

By knowing the ambient air temperature and humidity enthalpy of inlet air can be determined by using Eq. (6). For various mass flow rates, hole diameter and water depth, the enthalpy of outlet humid air from the humidifier can be determined by using Eq. (13). By trial and error method the exit specific humidity of the air can be calculated using Eq. (6).

Humidifier efficiency is the ratio between actual changes in specific humidity to the maximum possible specific humidity difference.

$$\eta = \frac{\omega_{2,\text{act}} - \omega_1}{\omega_{2,\text{sat}} - \omega_1} \times 100 \quad (14)$$

Effectiveness is used to measure the performance of the dehumidifier and it is given by:

$$\varepsilon = \frac{Q_{\text{actual}}}{Q_{\text{max}}} \quad (15)$$

Gained output ratio (GOR) is a dimensionless ratio defined as the ratio of the total latent heat of evaporation of the product water to the input thermal energy.

$$\text{GOR} = \frac{\dot{m}_e h_{fg}}{Q_{\text{in}}} \quad (16)$$

#### 4. Error analysis

At the humidifier inlet and humidifier outlet, to find the mass flow rate of hot moist air digital anemometer is used. Pressure gauges (0–500 psi) are attached at the condenser inlet and outlet to measure the pressure and also compound gauges (–30–250 psi) are connected to the evaporator inlet, evaporator outlet, and dehumidifier outlet. They measure the gauge pressure of the refrigerant. Mercury thermometer (–10°C–110°C) is placed at condenser inlet, condenser outlet, evaporator inlet, evaporator outlet, dehumidifier outlet for the refrigerant. For measuring relative humidity, wet and dry bulb thermometers are used. The energy meter, voltmeter and ammeter are used to measure the overall power consumption. A measuring beaker of 1 L is used for collecting pure distillate. The stopwatch is used for finding the total running time of the experimental setup. Uncertainty in a measured value can be defined as the chance of error occurred in the measured value of the instrument. In metrology, measurement uncertainty is the expression of the statistical dispersion

of the values attributed to the measured quantity. It can be found using the following formula [16]. Table 1 represents the accuracy and uncertainty of the various measurements.

$$\text{Uncertainty} = \left( \frac{\text{Accuracy}}{\sqrt{3}} \right) \quad (17)$$

#### 5. Results and discussion

The first set of experiments are carried out to examine the impact of the mass flow rate of air on the COP of the refrigerator. Water temperature in a humidifier is held approximately constant at 70°C by adjusting the fuel supply in the biomass stove. Five different mass flow rates of 6.77, 8.62, 9.85, 10.78 and 12.32 kg/h are used in experimentation. It is observed from the graph (Fig. 6) that increases in mass flow rate increase the COP. This is because as the mass flow rate of air increases, the heat capacity (mass flow rate × specific heat of air) will increase and thus moisture absorption capacity of the air in the humidifier chamber due to a reduction in relative humidity during heating. Also, more distillation was another output. This increase in COP accelerated as the water level is increased in the humidifier. This is due to more retention time as the air travels more depth along the water surface. The maximum obtained COP is 6.8 for the mass flow rate of inlet air of 12.32 kg/h at a water depth of 20 cm in a humidifier. Depends on the capacity of the humidifier chamber and blower speed the water depth is limited to 20 cm.

The sub-cooling of refrigerant in the condenser and superheating of refrigerant in the evaporator augments the COP of the system. Fig. 7 shows the P-h diagram of the improved system.

Table 1  
Uncertainty and error analysis

S. No.	Instruments	Accuracy	Range	Uncertainty
1	Compound pressure gauge	±5 psi	0–500 psi	2.89 psi
2	Pressure gauge	±1 psi	–30–250 psi	0.58 psi
3	Thermometer	±1°C	–10°C–110°C	0.58°C
4	Stopwatch	0.01 s	0–99 h	0.005 s
5	Measuring jar	±10 ml	0–1,000 ml	5.8 ml
6	Voltmeter	±10 V	0–300 V	5.77 V
7	Ammeter	±1 A	0–20 A	0.58 A
8	Energy meter	±0.1 kWh	0–10,000 kWh	0.06 kWh
9	Digital anemometer	0.01 km/h	0–50 km/h	0.005 km/h

Table 2  
Comparison the results with literature

Reference	System	Gained output ratio
[16]	Bubble column – HDH desalination – direct air	0.6
[16]	Bubble column – HDH desalination – preheated air	0.95
Present work	Bubble column – HDH – preheated air and preheated water	0.82

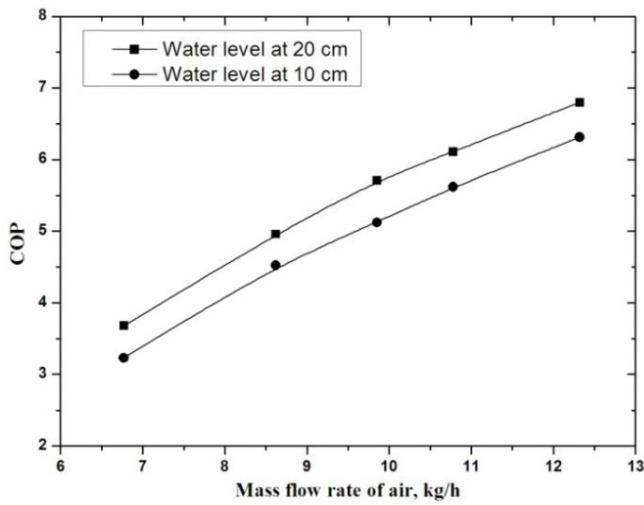


Fig. 6. Air mass flow rate effect on COP of VCR system.

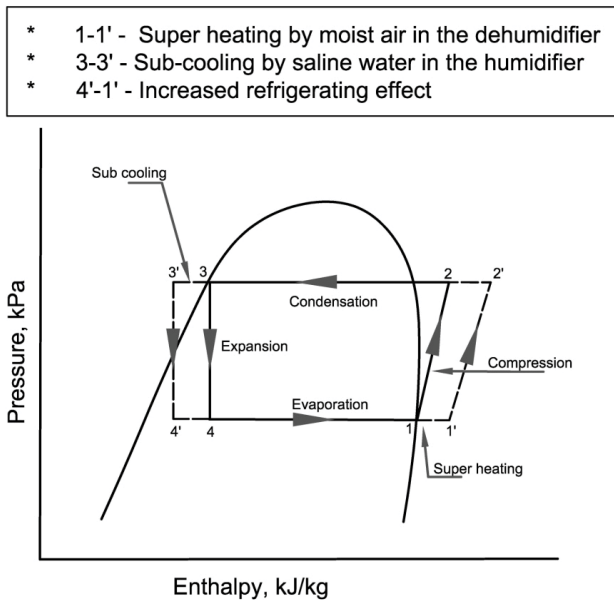


Fig. 7. Pressure-Enthalpy diagram for the proposed system.

Variation of specific humidity for various water temperatures in the humidifier chamber for different mass flow rates of air is given in Fig. 8. Three mass flow rates have been chosen for study with two water depth of 20 cm and 10 cm. Results show that an increase in water temperature causes improvement in water extraction in the humidifier. It is also observed that the specific humidity of moist air reaches a maximum of 88.61 g/kg of dry air at 70°C for a higher mass flow rate of 12.62 kg/h and a higher water depth of 20 cm. The amount of extracting water vapor is higher for a water depth of 20 cm compared to 10 cm. This is due to the fact that air retention time increases with the increase in water depth. Also, the increase in mass flow rate triggers the increase in the number of air bubbles that raise the rate of the interfacial area which in turn improves the amount of water extraction rate. So, humidification of air will be more,

and the mass flow rate of inlet air has an influence on the rise in specific humidity. Depends on the resulting maximum mass flow rate of 12.32 kg/h and water temperature of 70°C is fixed for further experimentation.

Based on the performance, the highest possible temperature of 70°C is maintained for further experimental work. Fig. 9 illustrates the relationship between mass flow rate air and specific humidity of humidifier outlet air for the two different water depths and at a constant water temperature of 70°C. Moist air capacity increases with increases in the mass flow rate of air due to enhanced heat capacity. The maximum specific humidity of 118.53 g/kg of dry air was attained at a water depth of 20 cm and for a mass flow rate of 12.62 kg/h. Theoretical specific humidity of air at humidifier outlet is calculated by using Eq. (13). Theoretical results to validate the experimental values have good agreement with below 10% deviation.

The effect of distillate rate on mass flow rate and water temperature is shown in Fig. 10. As the mass flow rate of inlet air and water level in humidifier surges, the distilled water output increases. When the water level is increased, air retention time (contact time between air and water) in the humidifier increases. So, air specific humidity is increased which leads to a rise in distilled output. When the air mass flow rate is accelerated, humidification is more which increases the distillate produced. To minimize the air-speed for enhancing retention time in a dehumidifier, rectangular inserts are attached in the middle pipe. As mentioned earlier, more water temperature in humidifiers causes more heat transfer between air and refrigerant which results in a higher distilled output. The maximum distilled obtained was 1.05 L/h for the water temperature of 70°C and depth of 20 cm.

Fig. 11 shows the system performance in terms of humidifier efficiency, dehumidifier effectiveness, gained output ratio, and cost of distilled water. The humidifier efficiency is higher than 90% for most of the flow rate. It shows the maximum saturation of air with water particles. This is due to the direct mixing of air with water by penetrating the water particles. The increase in flow rate enhances the mixing and it leads to higher humidifier efficiency. Dehumidifier effectiveness ranges between 0.51 and 0.6. The effectiveness decreases with the increase in air flow rate. Since the refrigerant flow rate is not varied, whereas the heat that needs to be removed increases with the flow rate and resulted in a decrease in effectiveness. Gained output ratio (GOR) of the biomass desalination system is low due to the waste heat leaving the atmosphere in the form of flue gas. The proposed system can produce the distilled water at a cost of 0.067 \$/kg for a flow rate of 12.32 kg/h.

The gained output ratio of the present work is compared with the previous biomass study results in Table 2. It shows that the GOR of the present system is comparable with the previous work. GOR of the biomass unit can be improved by effectively utilizing the waste heat to heat the air and water used for the HDH system.

The biomass stove in the integrated system releases the pollutant to the atmosphere in the form of flue gas. There is a need to extend the research to reduce the pollutant by introducing filters at the biomass outlet. Also, this system can be remodified by replacing the biomass stove with industrial waste heat from a recovery system or utilizing the

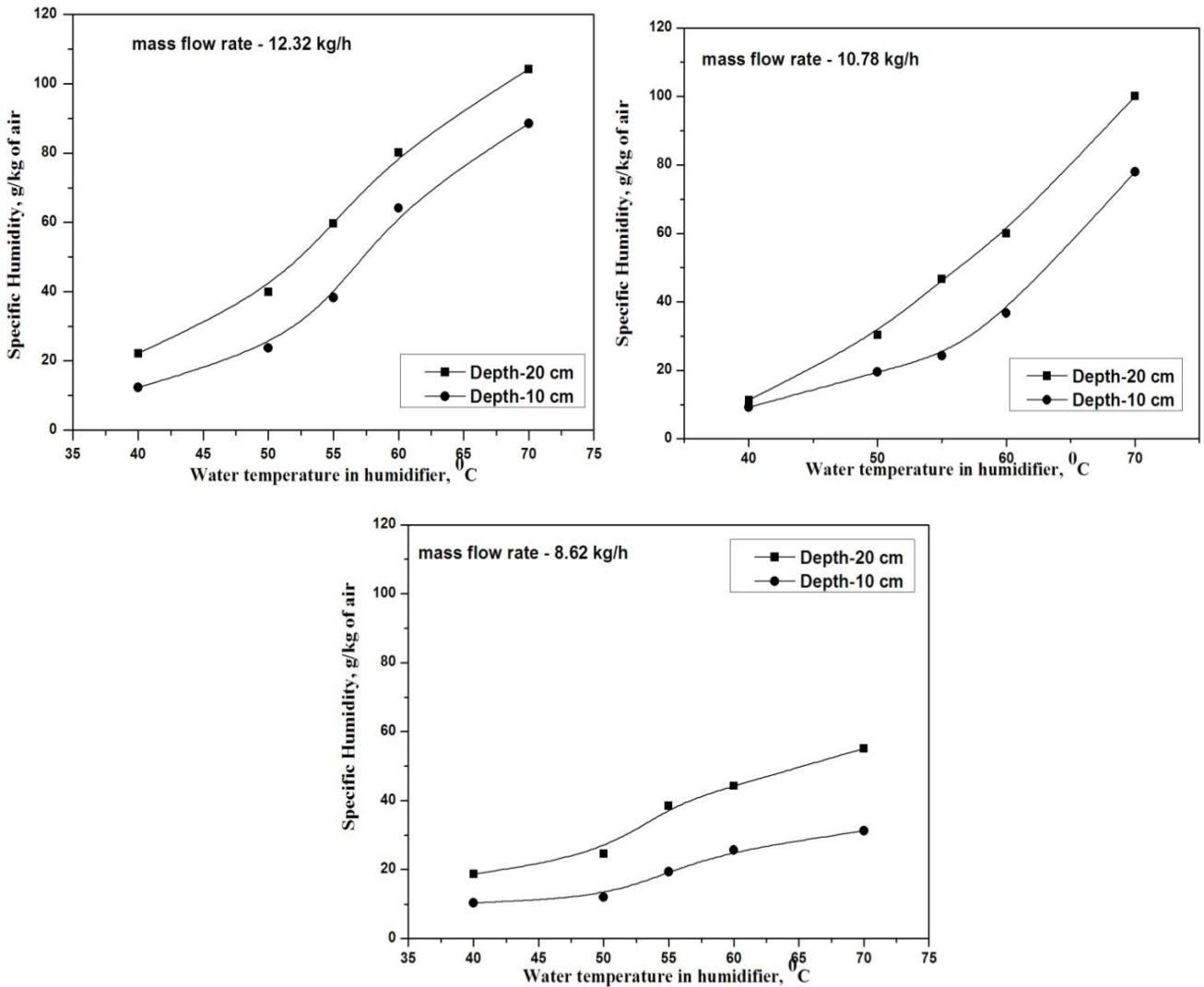


Fig. 8. Influence of water temperature, water depth and air mass flow rate on air specific humidity.

waste heat from internal combustion engines. In this way, the waste heat can be effectively utilized, and the overall system performance can be improved.

**6. Conclusion**

Integrating the VCR system along with biomass-operated bubble column humidification–dehumidification desalination system the COP of the VCR system is increased to 6.8 whereas the COP of the conventional VCR system is 4. The power required to run the blower (250 W) which is 0.54 times greater than the conventional setup (462 W). In the desalination system, five different mass flow rate of air is tested along with varying the five different water temperature and two different water depth. The maximum COP of the system is 6.8 for a mass flow rate of air of 12.32 kg/h, the water temperature of 70°C and water depth of 20 cm. The maximum distilled water observed was 1.05 L in the span of 1 h. Theoretical specific humidity is validated

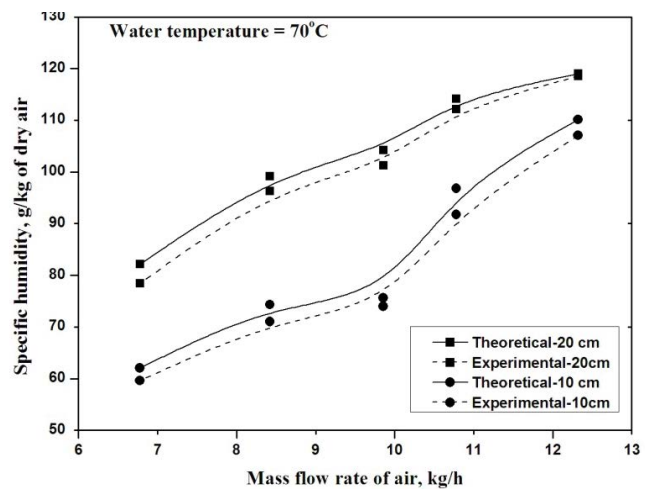


Fig. 9. Theoretical and experimental specific humidity variation.

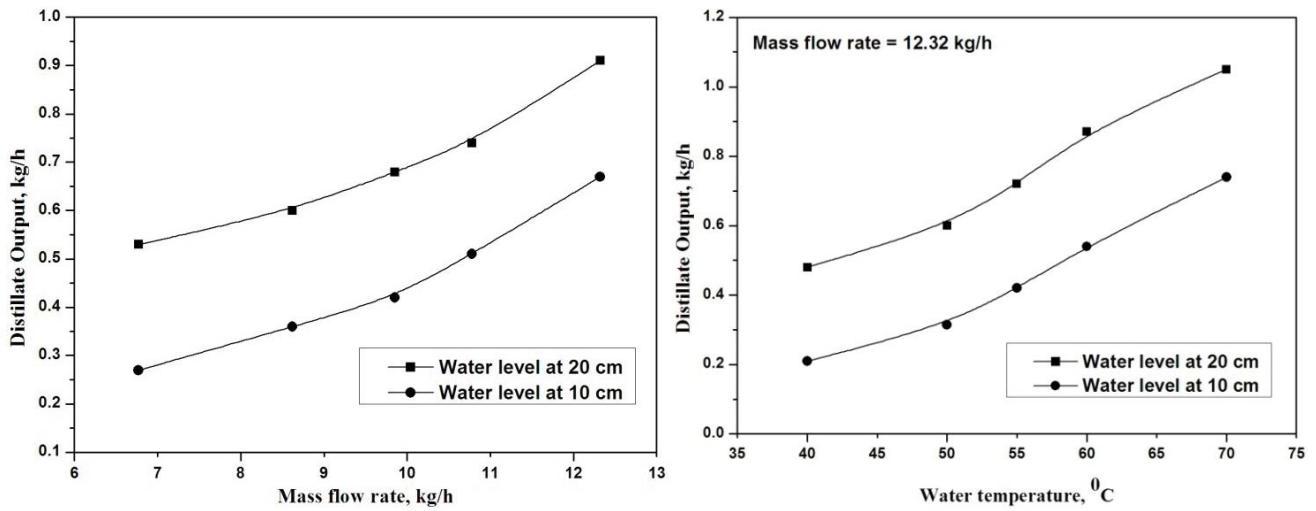


Fig. 10. Distillate output variation with (a) air mass flow rate and (b) water temperature.

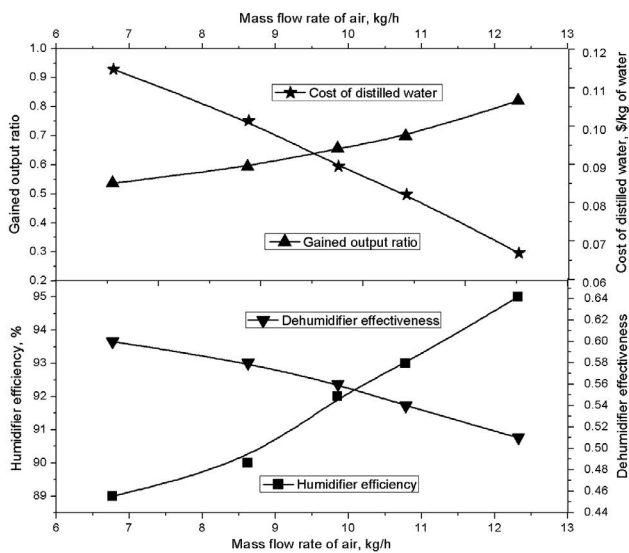


Fig. 11. System performance variation.

with experimental work. Within a range of 10%, theoretical results are coincide with the experimental results. For the optimum mass flow rate of 12.33 kg/h the proposed system can produce the distilled water at a cost of 0.067 \$/kg with the highest gained output ratio of 0.388. The humidifier efficiency reaches the maximum value of 95% and the maximum dehumidifier effectiveness of 0.6.

**Acknowledgment**

The authors would like to acknowledge with appreciation, Indian Society of Heating, Refrigeration and Air-conditioning Engineers (ISHRAE), India and ISHRAE, Madurai Chapter for the financial support for this analysis through Research in ISHRAE Project Grant and Thiagarajar College of Engineering, Madurai, India for their tremendous support to successfully deliver this project.

**Symbols**

- $A$  — Water surface area,  $m^2$
- $a$  — Specific interfacial area,  $1/m$ ,
- $C_p$  — Specific heat capacity of air,  $kJ/kg\ K$
- $D_{AB}$  — Diffusion co-efficient,  $m^2/s$
- $d_b$  — Bubble diameter,  $m$
- $d_o$  — Hole diameter,  $m$
- $E$  — Energy,  $kW$
- $H$  — Enthalpy,  $kJ/kg$
- $g$  — Gravitational acceleration,  $m/s^2$
- $h$  — Heat transfer co-efficient,  $kW/m^2\ K$
- $h_1$  — Enthalpy at compressor inlet,  $kJ/kg$
- $h_2$  — Enthalpy at condenser inlet,  $kJ/kg$
- $h_3$  — Enthalpy at condenser outlet,  $kJ/kg$
- $h_4$  — Enthalpy at evaporator inlet,  $kJ/kg$
- $h_d$  — Mass transfer co-efficient,  $kg/m^2\ s$
- $h_f$  — Enthalpy of saturated water,  $kJ/kg$
- $h_g$  — Enthalpy of saturated water vapour,  $kJ/kg$
- $h_{fg}$  — Latent heat of vaporization,  $kJ/kg$
- $Le$  — Lewis factor
- $\dot{m}$  — Mass flow rate,  $kg/s$
- $Pr$  — Prandtl Number
- $Q$  — Refrigeration effect,  $kJ/kg$
- $Re$  — Reynold Number
- $T$  — Temperature,  $^{\circ}C$
- $V_s$  — Superficial velocity,  $m/s$
- $\dot{W}_c$  — Work input to the compressor,  $kJ/kg$
- $Z$  — Height of water in humidifier,  $m$

**Subscripts**

- 1 — Humidifier inlet
- 2 — Humidifier outlet
- $a$  — Dry air
- lat — Latent
- in — Inlet
- out — Outlet
- sen — Sensible
- $v$  — Water vapor
- $w$  — Water

### Greek letters

- $\varepsilon$  — Gas holdup  
 $\rho$  — Density, kg/m<sup>3</sup>  
 $\omega$  — Specific humidity, kg/kg of dry air  
 $\sigma$  — Surface tension of water, N/m

### References

- [1] P.H. Gao, L.X. Zhang, H.F. Zhang, Performance analysis of a new type desalination unit of heat pump with humidification and dehumidification, *Desalination*, 220 (2008) 531–537.
- [2] R.B. Lokapure, J.D. Joshi, Waste heat recovery through air conditioning system, *Int. J. Eng. Res. Dev.*, 5 (2012) 87–92.
- [3] J. Wang, B.L. Wang, W. Wu, X.T. Li, W.X. Shi, Performance analysis of an absorption-compression hybrid refrigeration system recovering condensation heat for generation, *Appl. Therm. Eng.*, 108 (2016) 54–65.
- [4] S. Chinguwa, C. Musora, T. Mushiri, The design of portable automobile refrigerator powered by exhaust heat using thermoelectric, *Procedia Manuf.*, 21 (2018) 741–748.
- [5] P. Saji Raveendran, S. Joseph Sekhar, Performance studies on a domestic refrigerators retrofitted with building-integrated water-cooled condenser, *Energy Build.*, 134 (2017) 1–10.
- [6] N. Javani, I. Dincer, G.F. Naterer, Thermodynamic analysis of waste heat recovery for cooling systems in hybrid and electric vehicles, *Energy*, 46 (2012) 109–116.
- [7] S.A. Nada, H.F. Elattar, A. Fouda, Experimental study for hybrid humidification–dehumidification water desalination and air conditioning system, *Desalination*, 363 (2015) 112–125.
- [8] K. Srithar, T. Rajaseenivasan, M. Arulmani, R. Gnanavel, M. Vivar, M. Fuentes, Energy recovery from a vapour compression refrigeration system using humidification–dehumidification desalination, *Desalination*, 439 (2018) 155–161.
- [9] A.E. Kabeel, M.H. Hamed, Z.M. Omara, S.W. Sharshir, Experimental study of a humidification–dehumidification solar technique by natural and forced air circulation, *Energy*, 68 (2014) 218–228.
- [10] A.M.I. Mohamed, N.A.S. El-Minshawy, Humidification–dehumidification desalination system driven by geothermal energy, *Desalination*, 249 (2009) 602–608.
- [11] F.A. Al-Sulaiman, M.I. Zubair, M. Atif, P. Gandhidasan, Salem A. Al-Dini, M.A. Antar, Humidification–dehumidification desalination system using parabolic trough solar air collector, *Appl. Therm. Eng.*, 75 (2015) 809–816.
- [12] W.F. He, L.N. Xu, D. Han, Parametric analysis of an air-heated humidification–dehumidification (HDH) desalination system with waste heat recovery, *Desalination*, 398 (2016) 30–38.
- [13] P. Behnam, M.B. Shafii, Examination of a solar desalination system equipped with an air bubble column humidifier, evacuated tube collectors and thermosyphon heat pipes, *Desalination*, 397 (2016) 30–37.
- [14] K. Srithar, T. Rajaseenivasan, Performance analysis on a solar bubble column humidification–dehumidification desalination system, *Process Saf. Environ. Prot.*, 105 (2017) 41–50.
- [15] H.F. Elattar, A. Fouda, S.A. Nada, Performance investigation of a novel solar hybrid air conditioning and humidification–dehumidification water desalination system, *Desalination*, 382 (2016) 28–42.
- [16] T. Rajaseenivasan, K. Srithar, An investigation into a laboratory scale bubble column humidification–dehumidification desalination system powered by biomass energy, *Energy Convers. Manage.*, 139 (2017) 232–244.
- [17] S. Rădulescu, L.I. Negoită, I. Onuțu, Analysis of the heat transfer in double and triple concentric tube heat exchangers, *Mater. Sci. Eng.*, 147 (2016) 172–177.
- [18] G.A. Quadir, S.S. Jarallah, N.J. Salman Ahmed, I.A. Badruddin, Experimental investigation of the performance of a triple concentric pipe heat exchanger, *Int. J. Heat Mass Transfer*, 62 (2013) 562–566.
- [19] A. Gooma, M.A. Halim, A.M. Elsaid, Enhancement of cooling characteristics and optimization of a triple concentric-tube heat exchanger with inserted ribs, *Int. J. Therm. Sci.*, 120 (2017) 106–120.
- [20] D. Lawal, M. Antar, A. Khalifa, S. Zubair, F. Al-Sulaiman, Humidification–dehumidification desalination system operated by a heat pump, *Energy Convers. Manage.*, 161 (2018) 128–140.
- [21] D.U. Lawal, M.A. Antar, A. Khalifa, S.M. Zubair, F. Al-Sulaiman, Experimental investigation of heat pump driven humidification–dehumidification desalination system for water desalination and space conditioning, *Desalination*, 475 (2020) 114199, <https://doi.org/10.1016/j.desal.2019.114199>.
- [22] B. Anand, S. Murugavelh, Performance analysis of a novel augmented desalination and cooling system using modified vapor compression refrigeration integrated with humidification–dehumidification desalination, *J. Cleaner Prod.*, 255 (2020) 120224, <https://doi.org/10.1016/j.jclepro.2020.120224>.
- [23] M. Faegh, P. Behnam, M.B. Shafii, A review on recent advances in humidification–dehumidification (HDH) desalination systems integrated with refrigeration, power and desalination technologies, *Energy Convers. Manage.*, 196 (2019) 1002–1036.
- [24] D.U. Lawal, N.A.A. Qasem, Humidification–dehumidification desalination systems driven by thermal-based renewable and low-grade energy sources: a critical review, *Renewable Sustainable Energy Rev.*, 125 (2020) 109817, <https://doi.org/10.1016/j.rser.2020.109817>.